Polymer 51 (2010) 1432–1436

Contents lists available at ScienceDirect

Polymer

journal homepage: www.elsevier.com/locate/polymer

A novel approach to predict the recovery time of shape memory polymers

M. Bonner [a], H. Montes de Oca [b], M. Brown [b], I.M. Ward [a,*]

[a] School of Physics & Astronomy, The University of Leeds, Leads LS2 9JT, UK
[b] Smith & Nephew, Group Research Centre, York Science Park, Heslington, York, YO10 5DF, UK

ARTICLE INFO

Article history:
Received 15 October 2009
Received in revised form
22 January 2010
Accepted 25 January 2010
Available online 2 February 2010

Keywords:
Shape memory polymer
Polymer physics
Recovery

ABSTRACT

In this paper a novel approach is presented for prediction of the recovery time for a shape memory polymer. The Transient Stress Dip Tests of Fotheringham and Cherry are used to determine the two parameters of a Kelvin–Voigt element. The characteristic retardation time of this element can then be calculated to predict the recovery time. It is shown that this approach is successful in predicting the recovery times for a shape memory polymer drawn and recovered under a range of temperatures. Furthermore it is shown that the ratio of the recovery stress to the draw stress is independent of the drawing conditions to a very good approximation.

1. Introduction

Recently there has been a surge of interest in shape recovering polymers and the community has adopted the term shape memory polymers (SMP). A review of the recent progress in SMP and some of their applications in medical and non-medical industries can be found elsewhere [1–3].

Several models have been proposed to describe the behaviour of SMPs, with two of the most recent being by proposed by Nguyen [4] and Chen [5,6], however these rely on constitutive equations and are hence quite complex and require significant experimental work to determine the relevant parameters.

The earlier work of Li and Larock [7] and Lin and Chen [8,9] proposed simpler models based on varying combinations of Maxwell and Kelvin–Voigt elements. These are easy to understand models, all of which can under the right circumstances collapse to a single Kelvin or Voigt element.

In this work we present a novel approach to predict the shape recovery time on the basis of a simple Kelvin–Voigt model shown in Fig. 1, using the transient stress dip tests of Fotheringham and Cherry [9] to determine the stress in each arm under a range of drawing conditions and hence calculate both the recovery time of the material and the recovery stress available. We also investigate the effect of processing conditions on the recovery stress of SMPs.

2. Theory

It is possible to use the Kelvin–Voigt model shown in Fig. 1 to describe with a good degree of accuracy the behaviour of a viscoelastic material such as a solid polymer above the glass transition temperature. In this model the forward flow stress is given by the combined stress in the two arms. For the shape recovery we assume that the stress is stored in the spring E_R during the drawing process. This element drives the dashpot η_R backwards, resulting in the material returning to its original dimensions like a rubber band. The total applied stress (σ_T) on the system is the sum of the stress in the two arms, thus

$$\sigma_T = \sigma_R + \sigma_v \tag{1}$$

where σ_R is the recovery stress (the stress in the spring E_R) and σ_v is the viscosity stress, the stress in the dashpot η_R.

This model is characterised by a recovery half life τ which is simply given by [10]

$$\tau = \frac{\eta_R}{E_R} \tag{2}$$

where τ is the recovery half life, η_R is the viscosity of the dashpot and E_R is the modulus of the spring. This recovery time is a half life, and so in order to predict the actual recovery time we need to add together seven of these half lives to achieve a recovery of over 99%, since τ_1 is the time required to recover to half of the initial extension, τ_2 is the time required for half the remaining extension (equal to one quarter of the original extension) to recover, τ_3 is the time

* Corresponding author. Tel.: +44 113 343 3808; fax: +44 113 343 3846.
E-mail address: i.m.ward@leeds.ac.uk (I.M. Ward).

0032-3861/$ – see front matter © 2010 Elsevier Ltd. All rights reserved.
doi:10.1016/j.polymer.2010.01.058

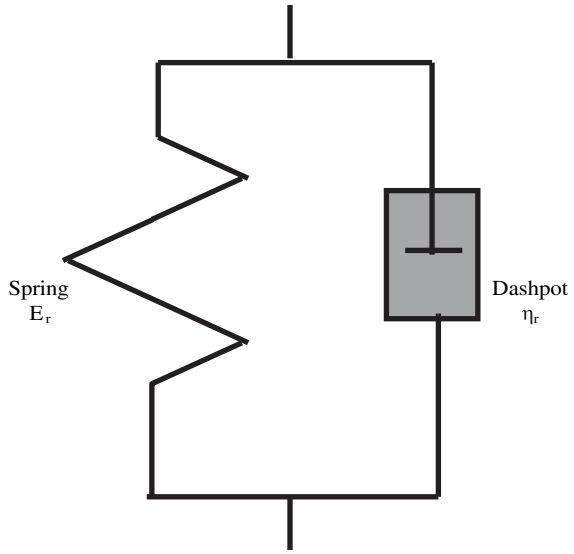

Fig. 1. Kelvin–Voigt model.

required for half the remaining extension (equal to one eighth of the original extension) to recover and so on. By adding together 7 of these half lives we obtain a total recovery of 99.2%.

In the first instance, in order to simplify the procedure, we will assume that we can simply multiply the recovery time by 7 to predict the overall recovery time (since to calculate the individual half recovery times would require data to be collected over a very wide range of conditions). Thus if a technique is available that allows the stress on the two arms to be determined then the recovery time can be calculated. We propose that the Transient Stress Dip Tests of Fotheringham and Cherry [9] are a suitable technique to separate the stresses on the two arms. In these tests a sudden and rapid reduction is strain is used to probe the stress level on the spring by observing the resulting behaviour of the load once the sample is held at constant strain. Because the total stress in the system is the sum of the stresses on the two arms it is then straight forward to calculate the stress on the dashpot. There are three possible situations schematically shown in Fig. 2 that can arise after the strain reduction has taken place.

i. $\sigma_T > \sigma_R$: In this case σ_v is positive and the stress reduces over time as the dashpot flows.
ii. $\sigma_T < \sigma_R$: In this case σ_v is negative and the stress increases over time as the dashpot flows.
iii. $\sigma_T = \sigma_R$: In this case the strain rate in the dashpot is zero and the stress initially remains constant with time.

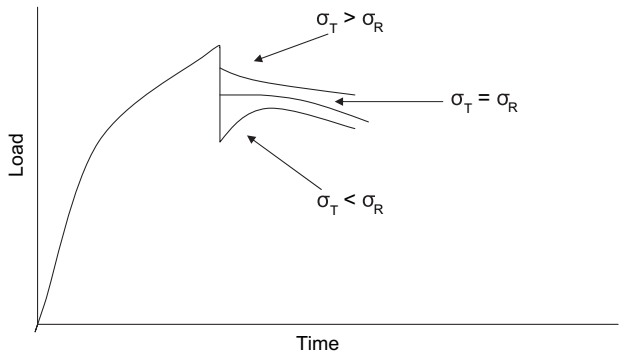

Fig. 2. Schematic representation of the three possible behaviours that can occur during the transient stress dip test.

Thus once σ_R has been determined E_R and η_R can be determined using the following equations:

$$E_R = \frac{\sigma_R}{\varepsilon} \tag{3}$$

and

$$\eta_R = \frac{\sigma_v}{\dot{\varepsilon}} \tag{4}$$

It is also apparent that for this approach to work the inherent stress relaxation of the material must be long compared to the shape recovery time. To confirm this, stress relaxation experiments were also performed.

3. Experimental methods

3.1. Materials

The material used in this work was based on an amorphous lactide based copolymer with 35% weight of calcium carbonate supplied by Smith & Nephew, York, in pellet form. This was converted to monofilament by using a bench scale melt spinning device attached to an Instron 5502. The spinning temperature was 160 °C, the die had an exit diameter of 2 mm and the crosshead was set to 2 mm per minute. The filament was spun into air at a rate of approximately 1 m per minute and allowed to coil into a clean tray for collection. There was a gap of approximately 1 m between the output of the die and the tray. This produced a monofilament of approximately 1 mm diameter. Because the material used degrades in the presence of water both the pellets and the monofilament were kept under vacuum when not being tested.

3.2. Initial drawing

Initial drawing experiments were performed to determine suitable conditions for later tests and also to ensure that the material exhibited suitable performance (i.e. complete recovery). These tests were performed on an Instron model 5502 using a long travel Instron environmental chamber to provide elevated temperature conditions. Drawing was performed over a range of temperatures (from 20 °C to 80 °C) and draw ratios (up to draw ratio 7).

3.3. Transient stress dip tests

Transient stress dip tests were performed on an Instron model 4505 utilising the advanced stress–strain panel to program the tests. The load output data from the Instron was monitored by a Pico ADC 200 linked to a laptop PC using Picolog software to record the data. In these tests a sample of length 75 mm (the maximum length possible for the sample to reach $\lambda = 4$ within the travel available in the oven) is extended under conditions of known crosshead displacement rate (equivalent to a nominal strain rate of 8.33×10^{-3} s^{-1}) to a predetermined strain (in this case up to a maximum of $\lambda = 4$). At this strain the crosshead is reversed a small amount at a strain rate that is at least 10 times that of the forward strain rate. Once the small amount of recovery has taken place the crosshead is held stationary and the load output is monitored as a function of time. The load was monitored until it was clear what behaviour the load was exhibiting. The tests were performed at elevated temperature by using an environmental chamber capable of controlling the temperature to ±2 °C.

3.4. Shape recovery tests

Recovery tests were performed on a dead loading creep rig (shown in Fig. 3), the output of which was monitored by computer using a data logging program written at Leeds. Samples for testing were prepared by drawing under the same conditions as for the transient stress dip tests (draw temperatures of 55–75 °C at a strain rate of 8.33×10^{-3} s^{-1}) to a draw ratio of $\lambda = 4$. The samples were prepared at least 24 h prior to the shape recovery tests being performed. Initial gauge lengths for the samples were between 80 mm and 100 mm. The environmental chamber was heated to the target temperature as quickly as possible (it took approximately 200 s from the start of the test for the air temperature in the chamber to achieve the set temperature) and held at the test temperature until the test was complete. The test was determined to be complete once the strain ceased to decrease and started to increase (i.e. once all the energy stored in the spring had been expended in recovery and the sample returned to an essentially isotropic state and started to creep in the normal manner).

3.5. Stress relaxation

Stress relaxation experiments were performed on an Instron model 5545. Isotropic samples were gripped and extended under conditions that were the same as those used for the transient stress dip tests. Once the sample reached $\lambda = 4$ (as determined by crosshead displacement) the crosshead was stopped and held stationary, whilst the load continued to be monitored.

4. Results and discussion

4.1. Initial results

It was found that for optimum shape memory performance to be observed (i.e. for near total recovery to be observed) then drawing temperatures of between 55 °C and 75 °C were required and a maximum draw ratio of $\lambda = 4$ could be imposed. Because of this for shape memory recovery tests were performed at a draw ratio of $\lambda = 4$, and transient stress dip tests were performed at draw ratios not exceeding $\lambda = 4$.

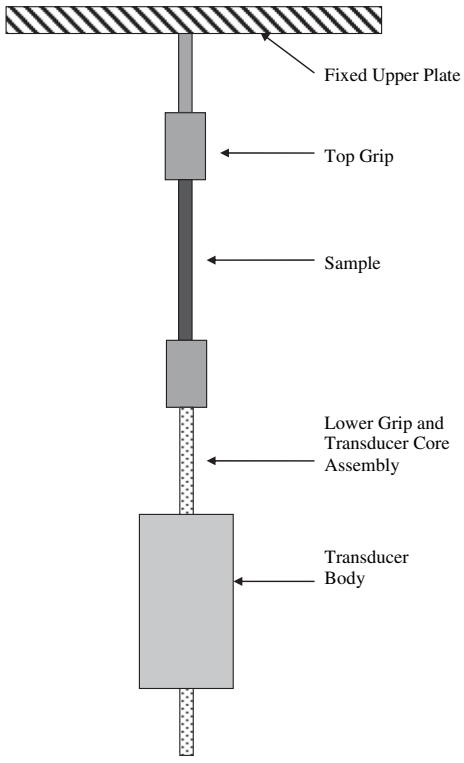

Fig. 3. Schematic diagram of a dead loading creep rig.

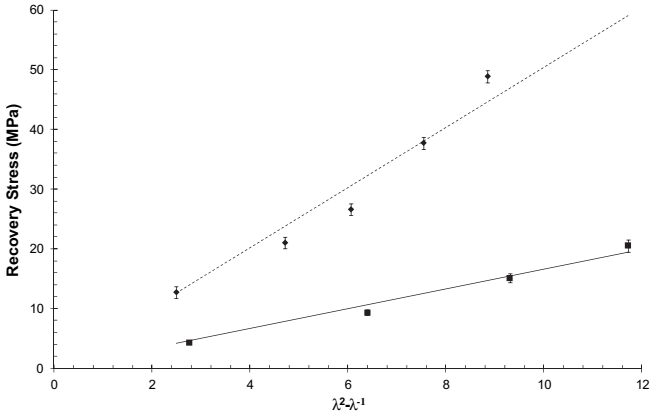

Fig. 4. Recovery stress against $\lambda^2 - 1/\lambda$ under tensile drawing at 55 °C and 65 °C. (Experimental data ◆ 55 °C, linear fit - - 55 °C, experimental data ■ 65 °C, linear fit – 65 °C).

4.2. Transient stress dip tests at varying draw ratios

The simplest explanation for the recovery force in a shape memory material is for the recovery force to be supplied by an internal recovery stress due to the recovery of an internal network which has been stretched in the drawing process [11].

$$\sigma_R = G\left(\lambda^2 - \frac{1}{\lambda}\right) \tag{5}$$

where G is an effective modulus for the material.

To test the validity of this equation transient stress dip tests were performed over a range of draw ratios at two different temperatures (55 °C and 65 °C) at a strain rate of 8.33×10^{-3} s^{-1}. Fig. 4 shows the recovery stress as a function of the draw ratio at 55 °C and 65 °C plotted against $\lambda^2 - 1/\lambda$. It is apparent that the material fits this model well. The G values determined from these curves for the two temperatures are 5.57 MPa for 55 °C and 1.82 MPa for 65 °C.

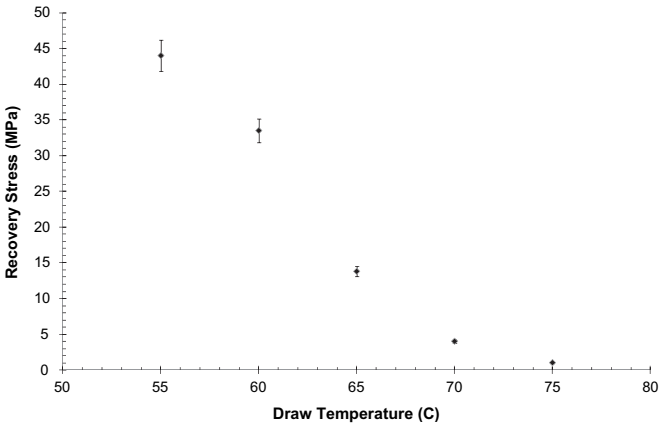

Fig. 5. Recovery stress as a function of draw temperature at $\lambda = 4$ and a strain rate of 8.33×10^{-3} s^{-1}.

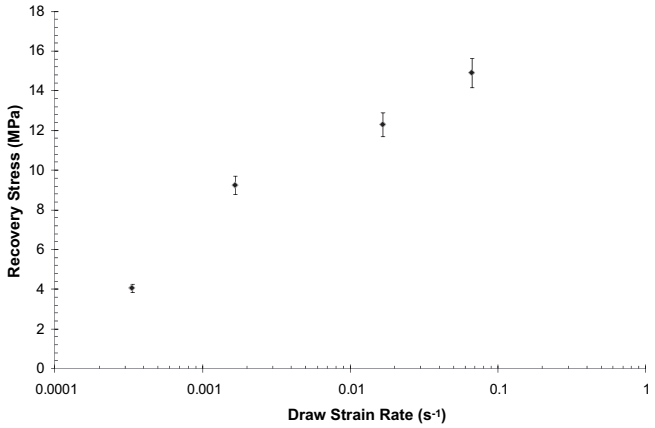

Fig. 6. Recovery stress as a function of strain rate at $\lambda = 4$ and 65 °C.

4.3. Transient stress dip tests at different temperatures and strain rates

Figs. 5 and 6 show the recovery stress as a function of draw temperature and strain rate respectively. Fig. 5 shows that the recovery stress decreases with increasing draw temperature and Fig. 6 shows that it decreases with decreasing strain rate.

Fig. 6 shows that the recovery stress has a linear relationship to the draw strain rate when plotted on a log scale. Fig. 7 shows that the viscosity stress has similar behaviour.

4.4. Ratio of the recovery stress to the total stress

Tests were performed to determine the ratio of the recovery stress to the total draw stress as a function of draw ratio, draw temperature and draw strain rate. The results showed that over the range of conditions studied (draw ratios from 1.5 to 4, temperatures of 55–75 °C and draw strain rates of $1.33 \times 10^{-4}\ s^{-1}$ to $1 \times 10^{-1}\ s^{-1}$) the ratio varies very little (from 0.7 to 0.8) and to a good first approximation can be considered constant at 0.75. For an elastic solid the ratio should be equal to 1 and a ratio of less than 1 is indicative of the viscoelastic behaviour of the material under consideration. At much higher drawing temperatures where the viscous component is expected to be dominant, the ratio should approach to zero, as the material loses its ability to store energy in the spring element of the Kelvin–Voigt model.

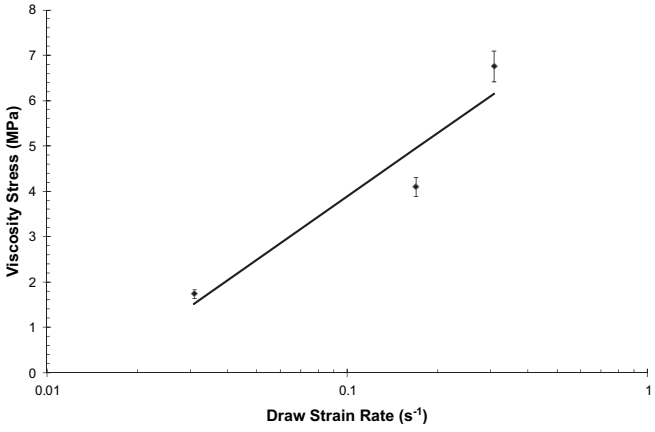

Fig. 7. Viscosity stress against $\log_{10}$ strain rate at 65 °C. (◆ experimental data, – linear fit).

Table 1
Predicted recovery times for the possible combinations of values compared to the experimentally determined recovery time for a sample drawn at 55 °C and recovered at 65 °C.

Combination	Predicted recovery time (s)	Actual recovery time (s)
$\frac{\eta_{Draw}}{E_{Draw}} = \frac{\eta_{55}}{E_{55}}$	1203	550
$\frac{\eta_{Recovery}}{E_{Recovery}} = \frac{\eta_{65}}{E_{65}}$	1291	
$\frac{\eta_{Draw}}{E_{Recovery}} = \frac{\eta_{55}}{E_{65}}$	3884	
$\frac{\eta_{Recovery}}{E_{Draw}} = \frac{\eta_{65}}{E_{55}}$	524	

4.5. Prediction of the recovery time

The data obtained from the transient stress dip tests allow the determination of the two components of the model E_R and η_R. However we must consider the appropriate combination of possible values to place into the equation. It would seem appropriate to consider the recovery stress as the recovery stress developed in the material during the deformation process, which is subsequently frozen into the material as the temperature is reduced below the glass transition temperature (T_g) of the process and the viscosity to be that determined at the recovery temperature. Table 1 shows that this is correct and that other combinations are not appropriate (all predicted times had 200 s added to them to account for the fact that the application of heat in the environmental chamber was not instantaneous).

To confirm this a series of recovery tests were performed using different drawing and recovery conditions, with the predicted recovery times being based on

$$\tau = \frac{\eta_{Recovery}}{E_{Draw}} \tag{6}$$

The results from these experiments are shown in Table 2 where it can be seen that in all cases there is good agreement between the experimentally determined and predicted times.

4.6. Stress relaxation

Fig. 8 shows that the time taken for the stress in the sample to decay to zero is of the order of several thousand seconds and therefore is long compared to the recovery process. These experiments indicate that in most practical situations the model will be valid, however as the shape recovery time approaches the stress relaxation time the model may start to break down since the internal stress will decay during recovery, leading to an extended recovery time. This may be the cause of the large under prediction seen in Table 2, where for material drawn at 65 °C and recovered at 55 °C the experimentally measured recovery time is 416 s longer than the predicted time of 3884 s. An examination of Fig. 8 shows that at 55 °C the internal stress has decayed to half of its original value after 3000 s. At present it is not currently possible to model these long term recovery situations since this requires the

Table 2
Predicted and actual recovery times for material drawn and recovered under a range of conditions.

Draw temp (°C)	Recovery temp (°C)	Predicted time (s)	Actual time (s)
55	55	1203	1030
55	65	524	550
55	75	216	212
65	55	3884	4300

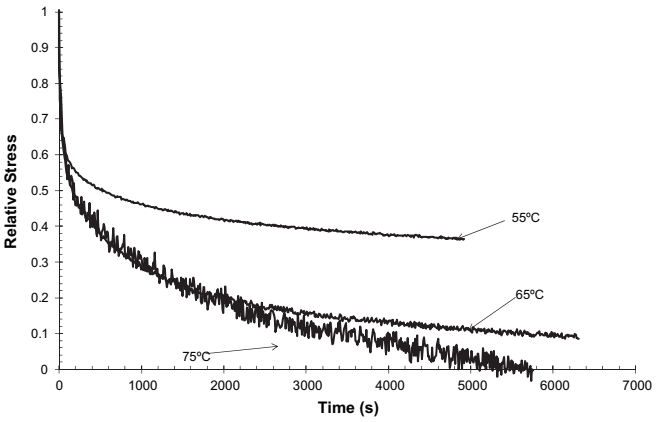

Fig. 8. Stress relaxation curves for material drawn at a nominal strain rate of 8.33×10^{-3} s^{-1} to $\lambda = 4$ at the temperatures shown.

determination of the viscosity term after stress relaxation, where we currently have no data.

5. Conclusions

A Kelvin–Voigt model combined with the Transient Stress Dip Test provides a simple yet powerful technique for predicting the shape recovery time of shape memory polymers (SMP), giving excellent agreement between prediction and experiment for recovery times of less than 1000 s and reasonable agreement for recovery times up to 4500 s. It was shown that shape recovery of SMP occurs when the spring component of the Kelvin–Voigt model or stored stress in the material exerts a force capable of deforming the viscous component or the dashpot element of the model at the temperature of shape recovery.

It was also found that the ratio of the recovery stress to the total stress is to a good approximation invariant for the three processing variables under consideration, namely drawing temperature, strain rate and draw ratio.

It is quite usual to describe the glassy stress–strain behaviour of polymers in terms of spring and dashpot elements. A common feature of such models involves a non-linear viscous dashpot, usually in series with a very stiff spring,in parallel with a weaker spring which provides strain hardening at high strains. The latter is often modelled by a rubber-like network, most simply a Gaussian network [12–16]. It is interesting that the spring element in the present investigation which relates to the internal stress, can also be described empirically by an affine deformation rubber elastic model although the deformation occurs in the glassy state below T_g. This result is consistent with the observations of Wendlandt et al. [17] who studied the development of segmental orientation in PMMA by NMR and showed that this followed the affine deformation model. The network structure for the number of Kuhn segments was however much smaller than the entanglement network found in the melt. Similar results were obtained by van Melick et al. [18] for the strain hardening modulus of polystyrene blends where it was shown that this decreased with increasing temperature as found in the present investigation.

It is not considered appropriate in this paper to pursue a detailed molecular interpretation of the results. Corrections to the apparent effective modulus of the recovery stress to take into account the filler content of 35 wt% calcium carbonate(modulus 35 Gpa [19]), using the method proposed by Chow [20], give corrected effective moduli of 3.55 Mpa and 1.12 Mpa at 55 °C and 65 °C respectively. Classical network theory, assuming appropriate molecular weights for the monomer components of the polymer, then predicts 15 and 43 monomer units between the junction points of the effective network at 55 °C and 65 °C respectively.

Following Fotheringham and Cherry [9] the viscosity stress can be considered to be a thermally activated process. Most simply it can be modelled by a single Eyring process with a strain rate dependence at high stress given by

$$\dot{\varepsilon} = \dot{\varepsilon}_0 \exp - \left(\frac{\Delta U - \sigma V}{kT} \right) \tag{7}$$

i.e.,

$$\ln \dot{\varepsilon} = \ln \dot{\varepsilon}_0 - \frac{\Delta U}{kT} + \frac{\sigma V}{kT} \tag{8}$$

Fig. 7 shows the experimental results at 65 °C from which a value for V of 5, 300 $Å^3$ is obtained, similar to results for polymers reported by Haward and Thackray [12], Truss et al. [21] and Fotheringham and Cherry [9] who did however consider it better to assume cooperative jumps of several chain segments and hence arrive at a smaller activation volume.

Acknowledgements

The authors wish to thank Yorkshire Forward and the Technology Strategy Board for their financial support during this work.

References

[1] Liu C, Qin H, Mather PT. J Mater Chem 2007;17:1543–58.
[2] Mather PT, Luo X, Rousseau IA. Annu Rev Mater Res 2009;39:445–71.
[3] Sokolowsky W, Metcalfe A, Hayashi S, Yahia L, Raymond J. Biomed Mater 2007;2:S23–7.
[4] Nguyen TD, Qi HJ, Castro F, Long KN. J Mech Phys Solids 2008;56:2792–814.
[5] Chen YC, Lagoudas DC. J Mech Phys Solids 2008;56:1766–78.
[6] Li F, Larock RC. J Appl Polym Sci 2002;84:1533–43.
[7] Lin JR, Chen LW. J Polymer Res 1999;6:35–40.
[8] Lin JR, Chen LW. J Appl Polym Sci 1999;73:1305–19.
[9] Fotheringham DG, Cherry BW. J Mater Sci 1978;13:951–64.
[10] Ward IM. Mechanical properties of solid polymers. 2nd ed. Chichester: Wiley; 1983.
[11] Treloar LRG. The physics of rubber elasticity. 3rd ed. Oxford: Clarendon Press; 1975.
[12] Haward RN, Thackray G. Proc Roy Soc Lond A 1968;302:453.
[13] Boyce MC, Parks DM, Argon A. Mech Mater 1988;7:15–33.
[14] Arruda EM, Boyce MC. Int J Plast 1993;9:697–720.
[15] Buckley CP, Jones DC. Polymer 1995;36:3301–12.
[16] Tervoort TA, Smit RJM, Brekelmans WAM, Govaert LE. Time Dependent Mater 1997;1:269–91.
[17] Wendlandt M, Tervoort TA, van Beck JD, Suter UW. J Mech Phys Solids 2006;54:599–610.
[18] van Melick HGH, Govaert LE, Meijer HEH. Polymer 2003;44:2493–502.
[19] Lutz JT, Grossman RF. Polymer modifiers and additives. CRC Press; 2000.
[20] Chow TS. J Mater Sci 1980;15:1873–88.
[21] Truss RW, Clarke PL, Duckett RA, Ward IM. J Polym Sci Polym Phys Ed 1984;22:191–209.